An Analysis of Radar Echo Systems for the Upper Midwestern United States

KENNETH B. MIELKE[1] AND DAVID D. HOUGHTON

Department of Meteorology, University of Wisconsin, Madison, Wisc. 53706

(Manuscript received 30 August 1976, in revised form 14 June 1977)

ABSTRACT

An extensive statistical study was made of the properties of radar echo systems in the upper Midwest region of the United States. Mesoscale groupings of echoes with distance scales 10–100 km and time scales 3–10 h instead of individual echoes were considered in the expectation that the former would be more relevant to deterministic short range prediction models.

A total of 203 case histories for 1974 was analyzed. Statistics for the area and duration were determined for the three categories of echo systems: those associated with warm fronts, with cold fronts and with neither. Correlations with the positions of the frontal zones and relationships with upper air winds were also made.

Consistent with earlier studies, it was found that the larger echo systems tend to last longer and that the direction of motion was usually somewhat to the right of upper level winds. Results provided many quantitative relationships that would be useful for prediction schemes and for developing models that carry mesoscale precipitation areas as explicit parameters.

1. Introduction

The basic motivation for this analysis was the improvement of short-range (0–24 h) precipitation forecasting techniques. Numerical and objective weather prediction models have proven useful for synoptic-scale, medium and long-range forecasts, but the prediction skill of short-range mesoscale forecasts is still less than adequate. The importance of these forecasts to the conduct of a wide spectrum of human activities cannot be overstated.

The study presented here provides a comprehensive statistical analysis of radar precipitation data over the upper Midwest in order to identify relationships useful as direct input into prediction models. Although many scales were represented by these data, it was found most desirable to focus on a scale of organization described as "echo systems." Echo systems, as defined in this analysis, are mesoscale features with a scale range of 10 to 100 km, composed of cells which form and retain a distinct structure on a radar scope from development to dissipation. After a careful time and space analysis, those echoes or echo clusters which appeared to be dynamically linked throughout their history were selected as echo systems. These are further defined in Section 2. The echo systems were divided into three major categories—those associated with warm fronts, with cold front and with neither (air mass). This study examines and compares various aspects of each echo system type including duration, horizontal dimensions, relationships to frontal zones and correlations with upper level winds.

The movement and predictability of radar echoes has been the topic of several reports in recent years. The focus in these investigations was primarily on individual echoes or severe convective activity with little emphasis on a detailed quantitative analysis and comparison of echo types. Cruz (1973) carried out a mesoscale experiment during 1969 in Venezuela in which 232 cloud histories were analyzed. In addition to computing several statistical properties, Cruz also examined the interrelationship of mesoscale and synoptic scale phenomena. Betts and Stevens (1974), also engaged in the Venezuelan experiment, collected 159 cloud histories during 1972. Statistical properties evaluated included lifetime, growth time, decay time, maximum area, maximum height of individual storms plus a qualitative discussion on echo movement. Austin and Houze (1972) did a detailed study of radar echoes observed in New England and attempted to analyze their larger mesoscale characteristics. Most of the analysis focused on the structures with dimensions of 30 km and less.

Digital radar data were utilized by Barclay and Wilke (1970) to isolate echo centroids and to extrapolate their movement through the use of computers. Particular emphasis was directed toward those properties of storms hazardous to aviation operations. These included diurnal variation of severe weather, surface wind shifts and gusts, and turbulence associated with

[1] Current affiliation: National Weather Service Forecast Office, Great Falls, Mont.

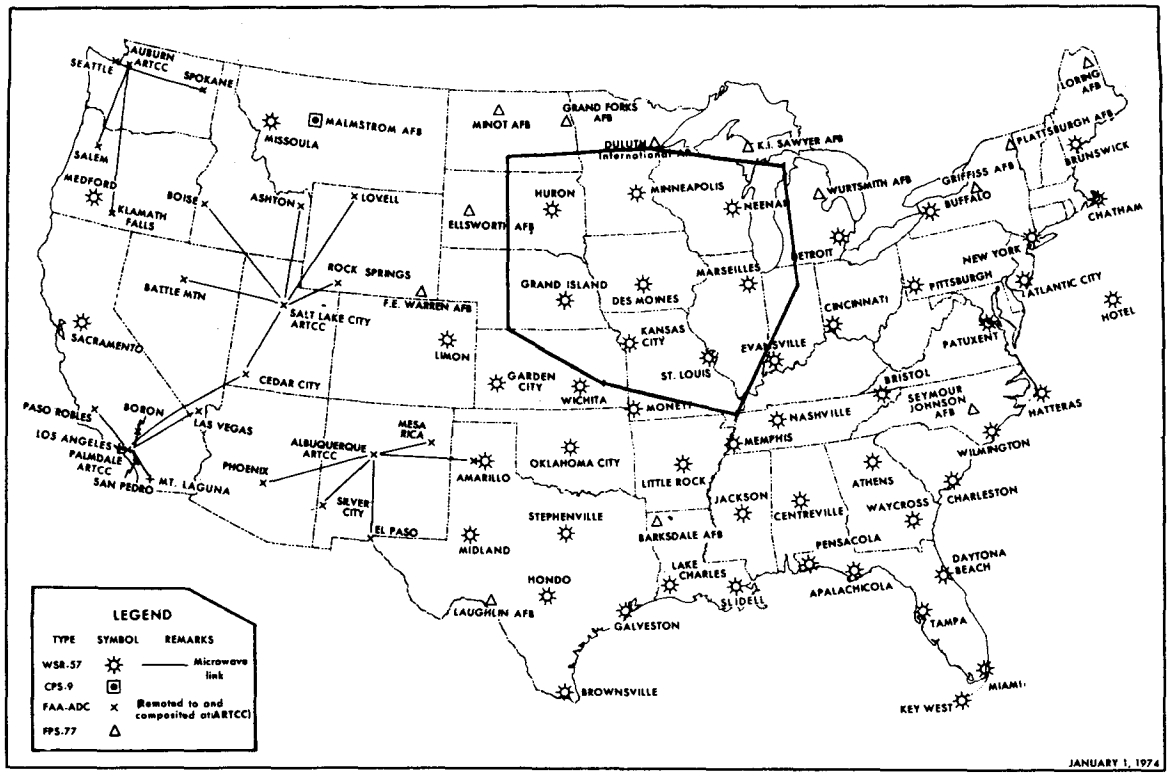

FIG. 1. Area of analysis in the upper Midwest including the location of the eight WSR-57 radar sites for the data.

severe storms. Wilson (1966) developed a cross-correlation technique utilizing quantitative radar data and computers to determine the movement and predictability of radar echoes. Echoes were classified according to the wavelength in the echo pattern. Wilson found the longer wavelength features to be the most predictable.

Newton and Fankhauser (1964) investigated the movement of storms over Oklahoma in a combined statistical-physical approach. Storms were classified according to horizontal dimensions and correlated with the mean wind in the cloud-bearing layer. They concluded that small storms more closely approached the mean 850–300 mb wind speed than did the larger storms. In addition, small storms deviated to the left of the mean wind, while large storms deviated to the right. The degree of deviation depended on how strongly the wind veered with height. They also investigated the movement of cells in case histories of large storms, storm complexes and squall lines.

2. Data and methods of analysis

The U. S. Department of Commerce 1974 *Daily Weather Maps* were utilized to identify active frontal systems and extensive precipitation areas for the upper midwest (see Fig. 1). This area of the United States was chosen because of the high frequency of frontal types and also because it contains a uniform radar network. After particularly active systems were identified, National Weather Service (NWS) WSR-57 radar films were procured for the days of interest.

Each radar film strip consisted of photographs of the PPI scope of the WSR-57 radar and was projected on a microfilm reader for analysis. To assure a degree of uniformity, only those echo histories with sufficient photographs to provide continuity were examined in this study. Although most histories consisted of photographs taken at least every 15 min, the preferred frequency depended on the duration of the echo system. Finally, only those photographs taken while the radar settings were at full power and minimum elevation were acceptable.

All echo systems which formed a distinct image or grouping and could be traced from initial development to dissipation on the same radar scope were analyzed. Included were systems composed of one or two cells ranging to systems containing four or five cells. Echo systems which merge and split were excluded. Fig. 2 illustrates the types of echo histories acceptable for this analysis. Panels *a* and *b* define merging and splitting echo systems which were not admissible. Represented in panels d and e are mesoscale line echoes which behave as an entity. In panel f an echo system group forms and decays as an entity, while in panel c sections of the group decay at different rates and do not appear to be dynamically linked.

A total of 203 echo system traces were analyzed.

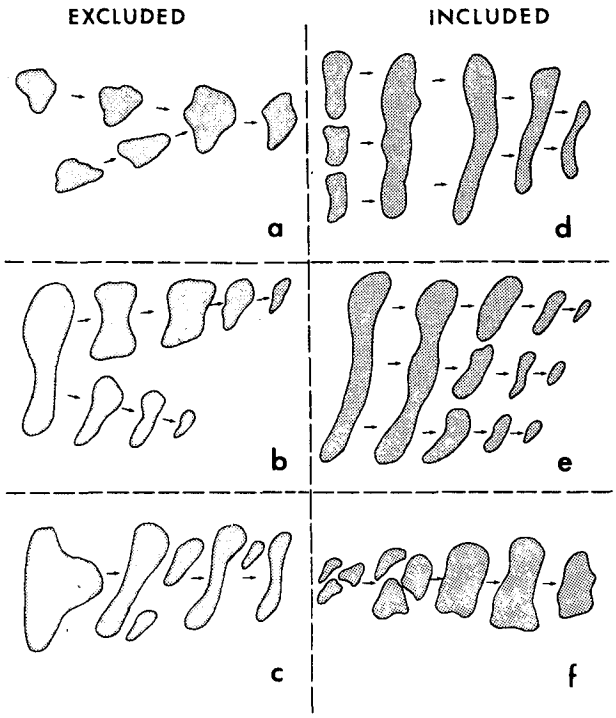

FIG. 2. Schematics of radar echo group evolution that were excluded from and included in the data set for echo systems used in this study. The enclosed areas represent actual echoes on the radar scope. See text for further discussion.

From each echo case history maximum area, duration, distance traveled, speed and mean direction of the echo system were computed. The mean direction of the systems was obtained by connecting a straight line from the center of the initial echo system image to the center of the final echo image. The length of this line divided by system duration yielded the speed. A fine-mesh transparent grid was produced to determine the maximum areas of the echo systems.

The echo traces were correlated with the proper NWS surface analysis corresponding to the same date and time. Echo systems were then subdivided into three basic categories: warm front, cold front and air mass. Upper level wind correlation with echo movement was accomplished from the radiosonde records. Since the location of the radiosonde data seldom coincided with the echo track, winds were often linearly interpolated, in time and space, from the surrounding stations.

3. Statistical properties of the echo systems

The mean maximum areas of the warm front, cold front and air mass echo systems were compiled with results depicted in Table 1. An analysis of the variance and subsequent significance tests performed on the means indicated that each echo type was significantly different in this parameter from the others at the 99% confidence level. The warm front echo systems were largest in mean maximum area, while the air mass systems displayed the smallest mean maximum area as would be expected.

The equivalent radius, as defined in Table 1, yields a better understanding of the size of the respective systems. This also serves as a reminder that the echo systems analyzed in this report are significantly larger in area than the individual cells treated in earlier investigations. Individual echoes analyzed by Cruz (1973) averaged 12.5 km in equivalent radius, while the radii of storms studied by Newton and Fankhauser (1964) ranged from a median of 9 km to a maximum of approximately 20 km. In Wilson's report (1966), a filtering technique was developed to isolate various wavelength features in convective storms. The wavelength categories ranged from a minimum of 9–15 km to a maximum of over 64 km. Most precipitation areas studied by Austin and Houze (1972) had equivalent radii <30 km. A few ranged up to 50 km. It should not be assumed, therefore, that if subsequent results differ from previous findings, that these results are contradictory.

Fig. 3 is a frequency distribution of echo maximum areas for each type of system. The distributions are highly skewed with a bias toward smaller values. The abscissa scales differ in each of the diagrams in Fig. 3 because of the wide range of maximum areas for each echo type. Classification categories were selected which enhanced detail in each echo type, while preserving statistical significance.

The mean echo system lifetime was 8.1, 5.6 and 3.9 h for warm front, cold front and air mass types, respectively. Significance tests performed on the means indicated that all three echo systems differed from one another at the 99% confidence level. For comparison, the average lifetime of air mass echoes in the Cruz (1973) study was less than 2 h, while the average lifetime was just over 2 h in the Betts and Stevens (1974) analysis and almost all were less than 3 h in the Austin and Houze investigation. Fig. 4 is a frequency distribution of echo system lifetimes. These graphs are more normally distributed than the area statistic just considered with a slight bias toward lower values. The difference in abscissa scales in this

TABLE 1. Echo system maximum area statistics. Equivalent radius was computed assuming the mean maximum areas were in the form of a circle.

Echo type	Mean ($\times 10^3$ km^2)	Standard deviation ($\times 10^3$ km^2)	Range ($\times 10^3$ km^2)	Equivalent radius (km)
Warm front (65 cases)	17.9	16.1	1.3–69.0	75.5
Cold front (85 cases)	10.6	9.7	0.3–44.0	58.1
Air mass (53 cases)	3.3	2.8	0.3–12.0	32.4

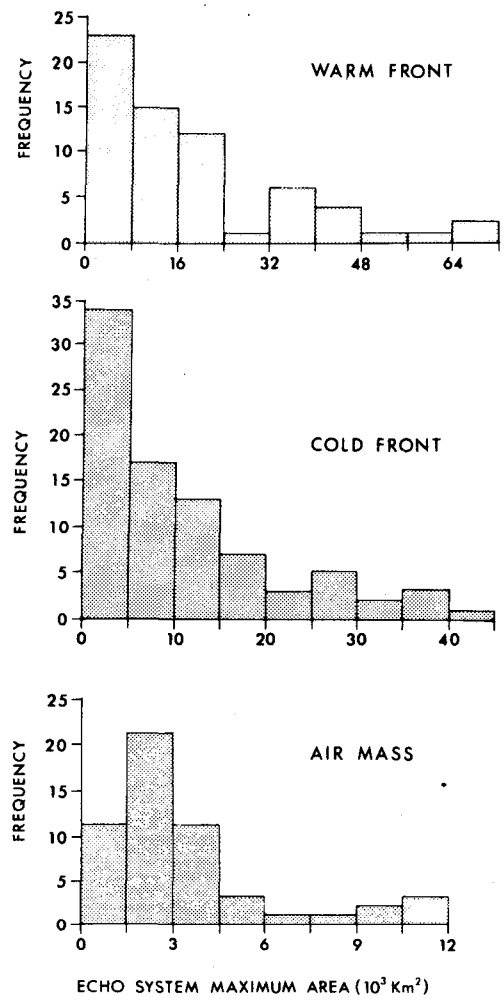

FIG. 3. Frequency distribution of echo system maximum areas in units of 10^3 km^2.

and subsequent frequency diagrams follows the same reasoning as discussed in the preceding paragraph.

Figs. 3 and 4 show that the warm front echo systems are significantly greater in maximum area and longer in lifetime. This is not unexpected, since warm fronts have typically shallow frontal slopes and are not as dynamically active as a cold frontal or air mass systems. Cold front echoes initially develop as a result of strong mechanical lifting which often leads to a vigorously convective system. Air mass echoes, due to mechanical lifting or solar heating, are also basically convective in nature. On the other hand, echoes in warm frontal zones, although convective at times, usually result from a broader, more gentle uplifting and thus are more steady state, which is consistent with the findings of this analysis.

Maximum area versus duration was plotted for each case according to echo type. A good correspondence was expected and attained. Fig. 5 displays the warm, cold and air mass maximum area versus duration plottings, respectively, together with the best-fit quandratic-regression equation curve. In all cases, there is a strong tendency for large echo systems to last longer. Cruz (1973) reached a similar conclusion for individual cells. However, for very large echo systems, the lifetimes tend to level off even as size continues to increase. Since the data base for the large echo system is rather small, no definite conclusion can be made.

The ratio of time to reach maximum area to total time of duration was computed for each individual history. The means and standard deviations of this ratio for each system type are given in Table 2. The peak near 0.50 shows the tendency for symmetrical echo histories. There were no significant differences between the cold front and warm front echo mean ratios considered separately. However, at the 95% confidence level, the mean ratio for both the cold and warm front echo systems was statistically different than the air mass system mean ratio. This suggests that an air mass system reaches its maximum area slightly before it reaches the midpoint of its life cycle. Furthermore, for a given duration, the time required to reach maximum area is less than that required for either a warm or cold front echo system.

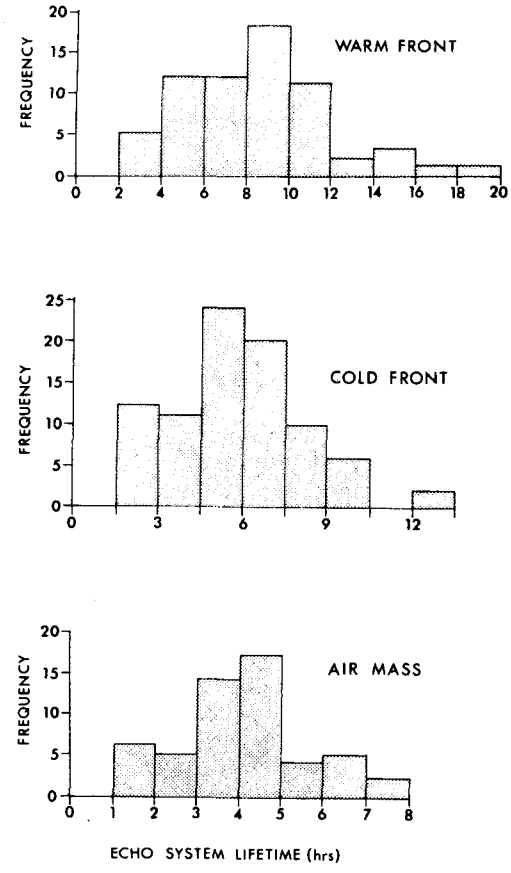

FIG. 4. Frequency distribution of echo system lifetimes in hours.

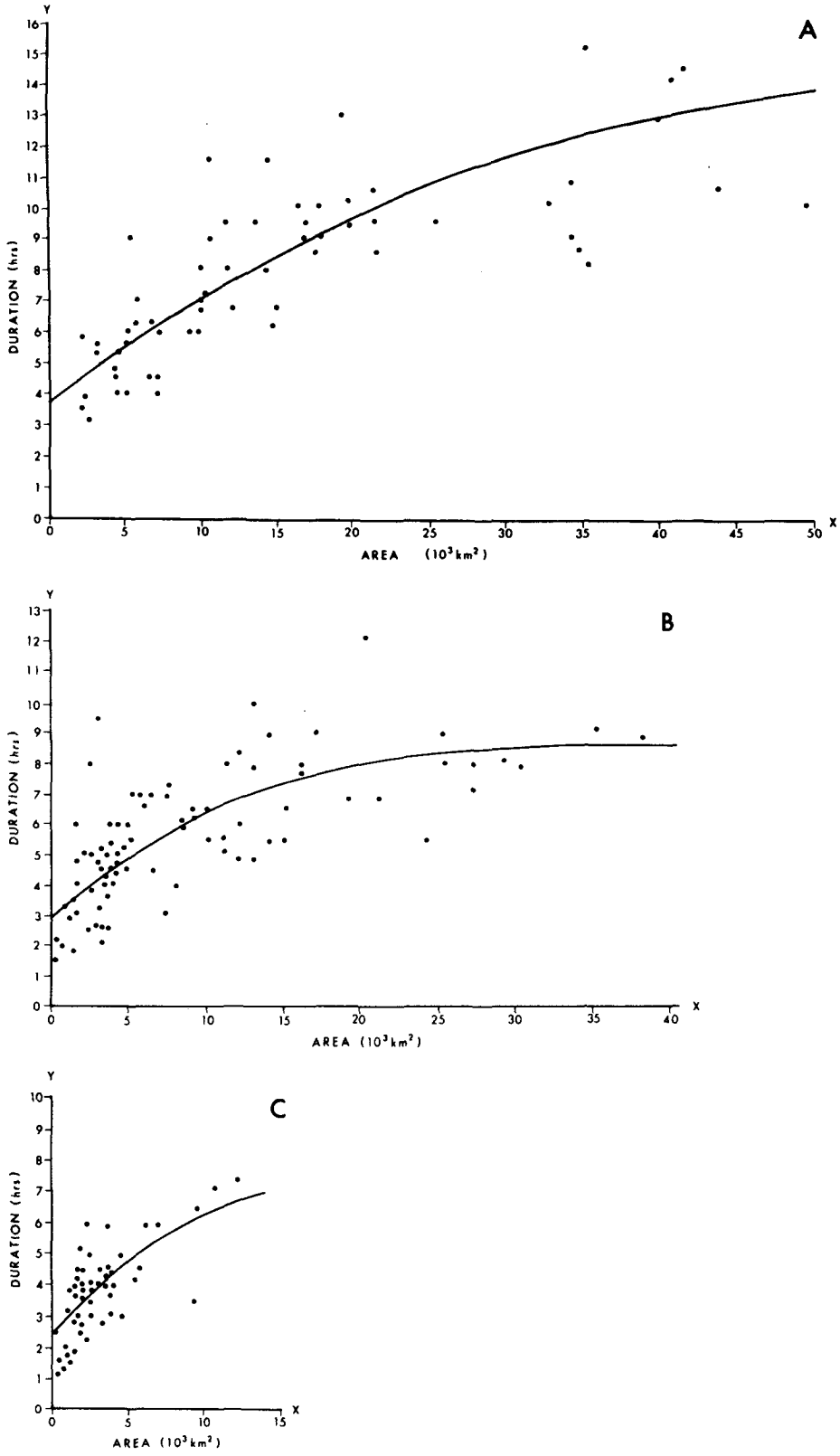

FIG. 5. Area versus duration for warm front, cold front and air mass echo systems in panels A, B and C, respectively. The best-fit quadratic-regression curve for each of the three cases is shown by the solid lines $y=3.724+0.348x-0.003x^2$, $y=2.984+0.359x-0.006x^2$, and $y=2.600+0.427x-0.008x^2$, respectively.

TABLE 2. Mean and standard deviation for the ratio of echo system time to reach maximum area to total time of duration.

Echo type	Mean ratio	Standard deviation
Warm front	0.50	0.08
Cold front	0.49	0.09
Air mass	0.45	0.10
Combined	0.48	0.09

4. Echo system distances from frontal zones

A total of 106 cases were analyzed to evaluate the relationship of echo systems to the analyzed surface front. NWS surface charts were procured as a reference. Distances were measured from the initial echo position to the surface front, which in many cases involved the linear interpolation of frontal movement. The mean echo system distance from the cold front was 19 km ahead of the front with a standard deviation of 45 km. In contrast, the mean echo system distance from the warm front was 80 km ahead of the front with a standard deviation of 67 km. Although a large standard deviation was evident in the cold front cases, 25 out of 56 of the echo systems were observed within 16 km of the frontal zone. In the warm front cases, however, the related echo system formations averaged well ahead of the analyzed surface front with a peak in the 80–120 km range. These results are not unexpected, since a warm front has a characteristically more shallow slope. A parcel mechanically lifted in a warm frontal zone must travel farther ahead of the surface front to achieve the equivalent lifting associated with a typically steeper cold frontal zone.

Some of the variance in echo system positions may be attributed to the analysis of the surface front position. The authors did not reanalyze the surface maps for possible frontal position error.

5. Upper level wind direction correlation

Using the 700, 500, 400–850, 400–700 and 300 mb winds obtained from rawinsonde records, directional departures of echo motion from the wind direction at each of the above pressure levels were calculated. The 400–850 mb layer-mean wind was derived by taking the 400 and 850 mb wind directions and computing a simple average. The 400–700 mb layer-mean wind was computed in the same manner. The means of the directional departures for each type of echo system are given in Table 3. All mean departures for the warm and cold front echo types ranged from 2.5° to 15° to the right of the wind direction. In contrast, the air mass mean departures ranged from 1° to 4° to the left of the wind direction in four of the five wind level classes.

The 500 and 300 mb wind levels for the warm front echo systems proved to be the most reliable predictors of echo motion with 80% of all echo systems moving within ±30° of these winds. About 89% of the echoes moved within ±30° of the 300 mb wind for the cold front echo systems, and the 400–700 mb layer mean wind closely followed with 88%. Finally, 95% of the air mass echoes moved within ±30° of the 700 mb wind. Frequency diagrams of these departures, uti-

TABLE 3. Regression equations, correlation coefficients, mean winds and standard deviations for direction of motion of each echo type as a function of wind direction at each wind level, ranked in order of highest correlation coefficients. Also given are mean echo system departure from observed wind.

Echo type	Wind level (mb)	Linear regression equation	Correlation coefficient	Mean direction of wind sample	Standard deviation of mean wind	Mean departure from observed wind
Warm front						
	500	$E_{dir}=0.86(500\ dir)+39°$	0.86	230°	41.7°	8.2°
	300	$E_{dir}=0.79(300\ dir)+53°$	0.84	237°	42.4°	2.5°
	400–700	$E_{dir}=0.73(400–700\ dir)+67°$	0.77	234°	42.7°	4.5°
	400–850	$E_{dir}=0.66(400–850\ dir)+90°$	0.66	226°	45.9°	12.9°
	700	$E_{dir}=0.52(700\ dir)+120°$	0.62	230°	50.1°	9.2°
Cold front						
	300	$E_{dir}=0.86(300\ dir)+40°$	0.94	242°	46.3°	6.9°
	400–700	$E_{dir}=0.85(400–700\ dir)+44°$	0.92	240°	43.8°	8.5°
	700	$E_{dir}=0.77(700\ dir)+65°$	0.91	235°	48.3°	12.1°
	500	$E_{dir}=0.80(500\ dir)+56°$	0.89	239°	45.5°	7.1°
	400–850	$E_{dir}=0.86(400–850\ dir)+47°$	0.89	234°	42.2°	14.6°
Air mass						
	700	$E_{dir}=0.87(700\ dir)+35°$	0.86	282°	36.5°	−4.1°
	400–700	$E_{dir}=0.81(400–700\ dir)+56°$	0.83	280°	38.0°	−2.3°
	400–850	$E_{dir}=0.78(400–850\ dir)+65°$	0.82	273°	39.6°	5.1°
	500	$E_{dir}=0.75(500\ dir)+68°$	0.79	277°	39.5°	−1.9°
	300	$E_{dir}=0.59(300\ dir)+116°$	0.75	282°	42.0°	−1.1°

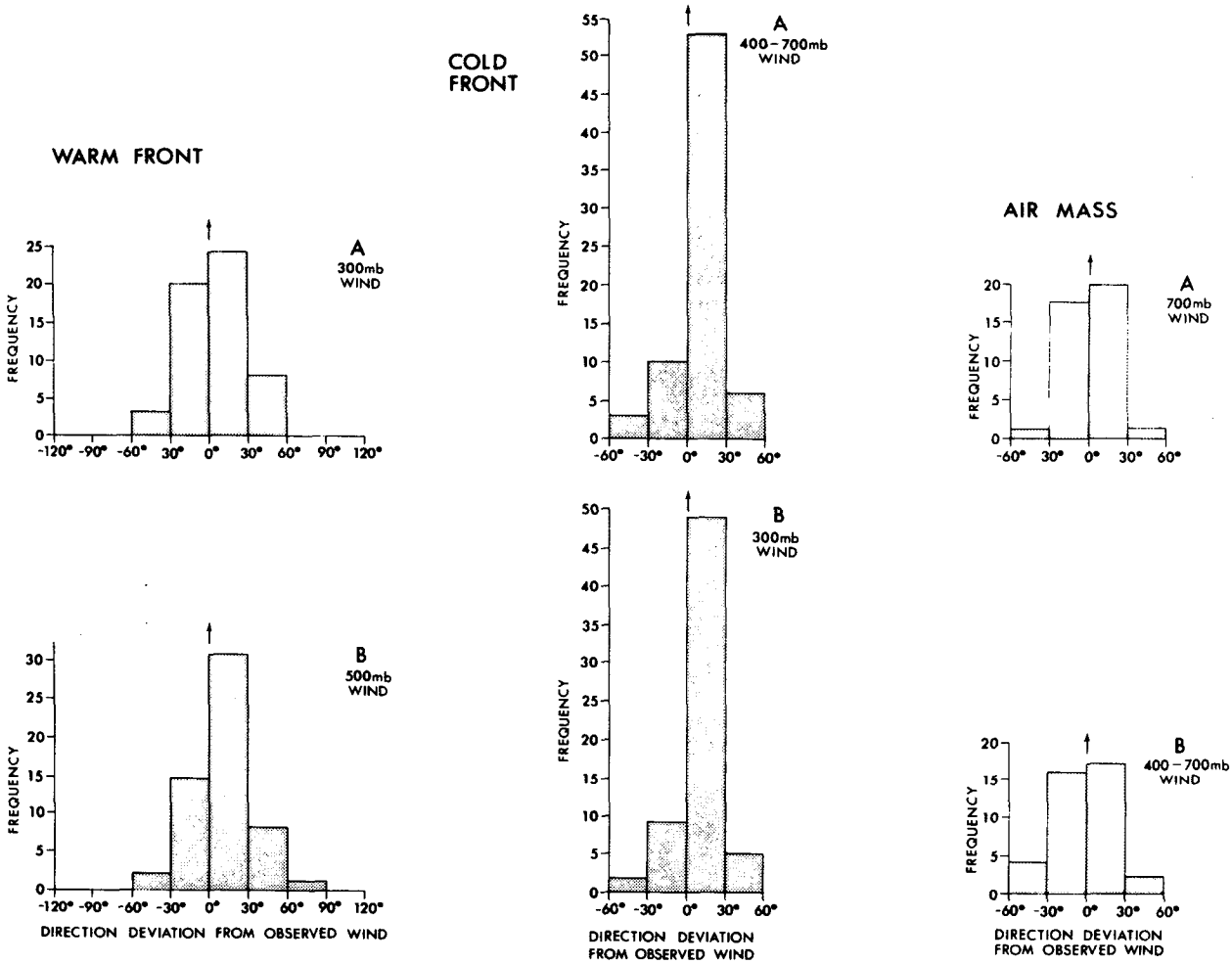

FIG. 6. Frequency distributions of echo system direction deviation (deg) from observed winds for selected wind level categories in the warm front, cold front and air mass situations as noted (left, center and right hand columns, respectively). The vertically pointing arrow emphasizes the abscissa position of the reference wind direction.

lizing the two wind level categories for each echo type which yielded the lowest standard directional deviation are depicted in Fig. 6. The tendency to move to the right of the mean wind is illustrated for the warm and cold front echo systems. The air mass echoes, however, show little preference. The 700 and 400–850 mb level winds were correlated with air mass echo direction by Cruz (1973) in Venezuela. While he found little in correlation between the two levels, in both cases, echo motion displayed a bias to the right of the wind direction.

Linear regression equations and correlation coefficients were calculated for echo motion direction as a function of wind direction at each of the five level categories with results as shown in Table 3. The mean wind directions and standard deviations are included in each sample to indicate where the equations are most applicable.

At least one good correlation coefficient was obtained in each case, although the cold front echo systems displayed high correlation coefficients with each of the wind levels. In a similar investigation Cruz (1973) computed a correlation coefficient of 0.70 in a comparison of 700 mb winds with air mass echoes in Venezuela. Newton and Fankhauser (1964), in a case study of several individual storm cells, computed a correlation coefficient of 0.66 using the 850–300 mb mean winds.

The 500, 300 and 700 mb level winds yielded the highest correlation coefficients for the warm front, cold front and air mass echo systems, respectively. Upon substitution of the mean wind directions given in Table 3, the regression equations respond with echo directional departures 4–14° to the right of the wind direction for warm and cold front systems. However, for the air mass systems, echo direction remains within ±5° of the wind direction, displaying no bias.

Using the median maximum area for each of the echo types, the echo systems were divided into two groups corresponding to large and small echo system

TABLE 4. Echo system direction as a function of wind direction with area as a parameter. For each echo type, only the wind level giving the highest correlation between wind and echo direction is considered. Also given, mean directional departure in degrees of echo system from observed wind.

Echo type	Wind level (mb)	Regression equation	Correlation coefficient	Number of cases	Area ($\times 10^3$ km^2)	Mean departure from observed wind
Warm front						
	500	$E_{dir}=0.92(500\ dir)+22°$	0.92	27	$\leqslant 10.0$	2.5°
		$E_{dir}=0.81(500\ dir)+55°$	0.74	30	>10.0	13.1°
Cold front						
	300	$E_{dir}=0.84(300\ dir)+42°$	0.96	30	$\leqslant 5.0$	3.5°
		$E_{dir}=0.93(300\ dir)+34°$	0.93	35	> 5.0	9.9°
Air mass						
	700	$E_{dir}=0.71(700\ dir)+86°$	0.76	21	$\leqslant 2.1$	−1.0°
		$E_{dir}=0.87(700\ dir)+28°$	0.92	21	> 2.1	−7.6°

areas. The median maximum areas were 10^4, 5.0×10^3 and 2.1×10^3 km^2 for the warm front, cold front and air mass echo types, respectively. The means and standard deviations of echo directional departures from the wind direction with area as a parameter were computed for each echo type.

The mean directional departures of the large echo systems were to the right of the small echo mean departures in all cases for the warm and cold front echo types. This was most evident at the 500, 400–850, 400–700 and 300 mb wind levels, where the large echo systems moved 5–12° to the right of the small echo systems utilizing the mean values of departures. In contrast, the large air mass echo systems exhibited a mean departure to the left of the small echo system mean departure ranging from 6° to 20°. Values of mean directional departures with dependence on area are given for one wind level for each echo type in Table 4.

In the study by Newton and Fankhauser (1964), small echoes (radius 5 km) generally moved to the left while large echoes (radius 15–20 km) moved to the right of the 850–300 mb mean wind. Two case histories of large storm clusters revealed that multicellular echoes deviated more to the right than large single-celled echoes. The results of the analysis qualitatively agree with the cold and warm front mean directional departure results of this study, even though the relative sizes of the respective echo categories differ significantly. The air mass echo systems, however, behaved in the opposite sense at each of the five wind levels considered.

Linear regression equations and correlation coefficients were computed for the large and small echo types, but only for the wind level of each echo type in Table 3 which displayed the highest correlation coefficient. These results are summarized in Table 4. The small warm and cold front echo systems correlated better with the upper level winds than the large echo systems, suggesting they may be more predictable. This was most significant in the warm front case. In addition, upon substitution of all winds within one standard deviation of the mean winds from Table 3, the regression equations yielded large echo system departures which were consistently to the right of the small system departures.

The air mass echo systems again displayed contrasting results. The large air mass echoes yielded a higher correlation coefficient than the small echo systems, suggesting that small air mass echoes are more erratic in direction of movement. Furthermore, upon substitution of winds within one standard deviation of the mean wind direction into the regression equations, the large echo systems consistently moved to the left of the small echo systems.

6. Upper level wind speed correlation

For each type of echo system, echo speeds were correlated with the 700, 500, 400–850 and 400–700 mb wind speeds. Echo system speed correlations with the 300 mb pressure level were excluded because of the 300 mb level's frequent proximity to the jet stream and consequential large isotach gradient which could result in large interpolation errors. The 400–850 mb wind speed was obtained by averaging the 400 and 850 mb wind speeds. The 400–700 mb wind speed was derived similarly. The means of echo speed departure were calculated for each echo type as shown in Table 5. In all cases the echo speed was less than the wind speed and there was little difference in speed departures among echo types for a given wind level. Considering the echo types collectively, echo speed was generally 25% less than the 700 mb wind speed and 40% less than the wind speed at the remaining levels.

Linear regression equations and correlation coefficients for echo speed as a function of wind speed are given in Table 5. Obviously, wind speed correlation

is more difficult to achieve than wind direction correlation. This also proved true in the Venezuelan study of air mass echoes by Cruz (1973). Using the 700 mb winds, he computed a correlation coefficient of 0.50.

Since the rawinsonde network is a synoptic grid scale, mesoscale wind speed variations were not always identified, which explains some of the variance in this aspect of the study. Wind direction fields, however, do not exhibit such large deviations at least at the synoptic scale and can be interpolated with a higher degree of accuracy.

Using the median maximum area, the data were divided into two groups of large and small echo system areas for each echo type. The means of echo speed departure from the wind speed were computed according to area. The large and small echo system speed departures differed very little and were similar to the values obtained in Table 5 at each respective wind level. Earlier investigators arrived at different results.

Wilson (1966) compared echo speed with the 3–6 km mean wind speed and found that small echo features moved at the speed of the mean wind while large echo features moved substantially slower. The radii of the echoes in his study ranged from 5 to 20 km. Newton and Fankhauser (1964), in a quantitative analysis, noted that small to medium size cells (radius 5–10 km) moved approximately 5% less than the 850–300 mb mean wind. The larger cells (radius 15–20 km) moved at a speed 25% less than this mean wind. This appears to contradict results shown in this report; however, the average radii of echo systems in this study range from 32 km for air mass systems to 75 km for warm front echo systems. Therefore, even the small echoes in this report average larger than the large cells of earlier investigations. The previous investigations suggested that as echo systems become larger, they tend to move slower than the mean wind field. In that respect, the results of this study qualitatively agree with earlier reports.

Linear regression equations were calculated for the data in Table 5 utilizing the two wind levels which yielded the highest correlation coefficients. These results, summarized in Table 6, indicate little significant changes in correlation coefficients for warm and cold front echo types with area as a variable. In the case of air mass echo systems, there is a significant difference between large and small echo system correlation coefficients. The large air mass echoes correlated fairly well, but the small echoes displayed almost no correlation with the wind level speeds. These results combined with results in Table 4 on wind direction correlation suggest that little success can be anticipated in predicting the speed and direction of small air mass echo systems.

Fig. 7 is a scaled schematic summary of Sections 5 and 6 displaying in vector form the mean values of motion for each echo system type. The 300 mb diagrams are not presented since echo speed correlations were not computed for this pressure level, as discussed in Section 6.

7. Conclusions and recommendations

Although there was great variability in all aspects of the echo systems, several significant conclusions about each type of echo system may be derived from this study. These are summarized below.

a. Warm front echo systems

1) Significantly larger in area and longer in duration than cold front or air mass systems.

TABLE 5. Regression equations and correlation coefficients of echo system speed as a function of wind speed at the specified levels, ranked in order of highest correlation coefficients. Also given, mean departures of echo speed from observed wind speed.

Echo type	Wind level (mb)	Linear regression equation (m s^{-1})	Correlation coefficient	Mean departure from observed wind (m s^{-1})
Warm front				
	400–700	$E_{speed}=0.40(400\text{–}700\ speed)+3.2$	0.62	−7.8
	700	$E_{speed}=0.33(700\ speed)+5.8$	0.56	−3.7
	400–850	$E_{speed}=0.37(400\text{–}850\ speed)+4.0$	0.50	−6.9
	500	$E_{speed}=0.25(500\ speed)+5.8$	0.43	−8.2
Cold front				
	500	$E_{speed}=0.33(500\ speed)+5.9$	0.56	−9.1
	400–700	$E_{speed}=0.37(400\text{–}700\ speed)+5.2$	0.53	−8.5
	400–850	$E_{speed}=0.36(400\text{–}850\ speed)+6.0$	0.46	−6.5
	700	$E_{speed}=0.25(700\ speed)+8.9$	0.38	−3.8
Air mass				
	400–700	$E_{speed}=0.31(400\text{–}700\ speed)+4.1$	0.60	−7.8
	700	$E_{speed}=0.34(700\ speed)+5.2$	0.59	−2.9
	500	$E_{speed}=0.31(500\ speed)+4.6$	0.56	−7.1
	400–850	$E_{speed}=0.29(400\text{–}850\ speed)+4.7$	0.56	−6.5

2) Displayed a symmetrical echo history.
3) Formed most frequently 30–45 km ahead of surface warm front.
4) Generally moved to the right of the mean wind; larger echoes moved further to the right.
5) Direction of movement correlated best with 500 mb mean wind direction; correlation coefficient 0.86. Correlation best with the smaller echoes.
6) Speed of movement correlated best with 400–700 mb wind level; correlation coefficient 0.62. Little dependence on area.

b. Cold front echo systems

1) Intermediate in maximum area and lifetime.
2) Displayed a symmetrical echo history.
3) Formation coincided with surface frontal position most frequently.
4) Generally moved to the right of the mean wind; larger echoes moved further to the right.
5) Direction of movement correlated well with wind directions at all levels; correlation coefficients 0.89–0.94. Smaller systems correlated best.
6) Speed of movement correlated best with 500 mb wind speed; correlation coefficient 0.56. Little dependence on area.

c. Air mass echo systems

1) Significantly smaller in maximum area and shorter in duration.
2) Reach maximum area before midpoint in life cycle.
3) Moved to the left of the mean wind in four of the five wind level categories; larger echoes moved further to the left.
4) Direction of movement correlated best with 700 mb wind; correlation coefficient 0.86. Larger echoes correlated best.
5) Speed of echo movement correlated best with the 400–700 mb wind and the 700 mb wind; correlation coefficients 0.60 and 0.59, respectively. Significantly size dependent; very poor correlation with small systems.

d. Characteristics common to all three systems

1) Good correlation of area vs duration in that larger echo systems tend to last longer.
2) Ratio of time to reach maximum area/duration vs maximum area increased with increasing maximum area of the systems.
3) Ratio of time to reach maximum area/duration vs duration increased with increasing duration of the systems.
4) The predictability of echo direction was better than the predictability of echo speed.

Although several definitive conclusions were obtained from the study, some points were left unresolved. The most limiting factor in this study was not the quality of data, but the quantity of data.

TABLE 6. Regression equations and correlation coefficients of echo system speed as a function of wind speed (m s^{-1}) with area as a parameter.

Echo type	Wind level (mb)	Regression equation (m s^{-1})	Correlation coefficient	Number of cases	Area ($\times 10^3$ km^2)
Warm front					
	400–700	$E_{speed}=0.45$(400–700 speed)$+2.6$	0.61	23	$\leqslant 10.0$
		$E_{speed}=0.34$(400–700 speed)$+4.1$	0.65	25	>10.0
	700	$E_{speed}=0.39$(700 speed)$+5.1$	0.56	23	$\leqslant 10.0$
		$E_{speed}=0.28$(700 speed)$+6.3$	0.60	26	>10.0
Cold front					
	500	$E_{speed}=0.29$(500 speed)$+6.8$	0.57	26	$\leqslant 5.0$
		$E_{speed}=0.41$(500 speed)$+4.2$	0.54	33	> 5.0
	400–700	$E_{speed}=0.37$(400–700 speed)$+4.7$	0.61	26	$\leqslant 5.0$
		$E_{speed}=0.39$(400–700 speed)$+5.0$	0.47	33	> 5.0
Air mass					
	400–700	$E_{speed}=0.10$(400–700 speed)$+8.2$	0.19	19	$\leqslant 2.1$
		$E_{speed}=0.39$(400–700 speed)$+2.9$	0.74	22	> 2.1
	700	$E_{speed}=0.16$(700 speed)$+7.9$	0.30	19	$\leqslant 2.1$
		$E_{speed}=0.41$(700 speed)$+4.1$	0.70	24	> 2.1

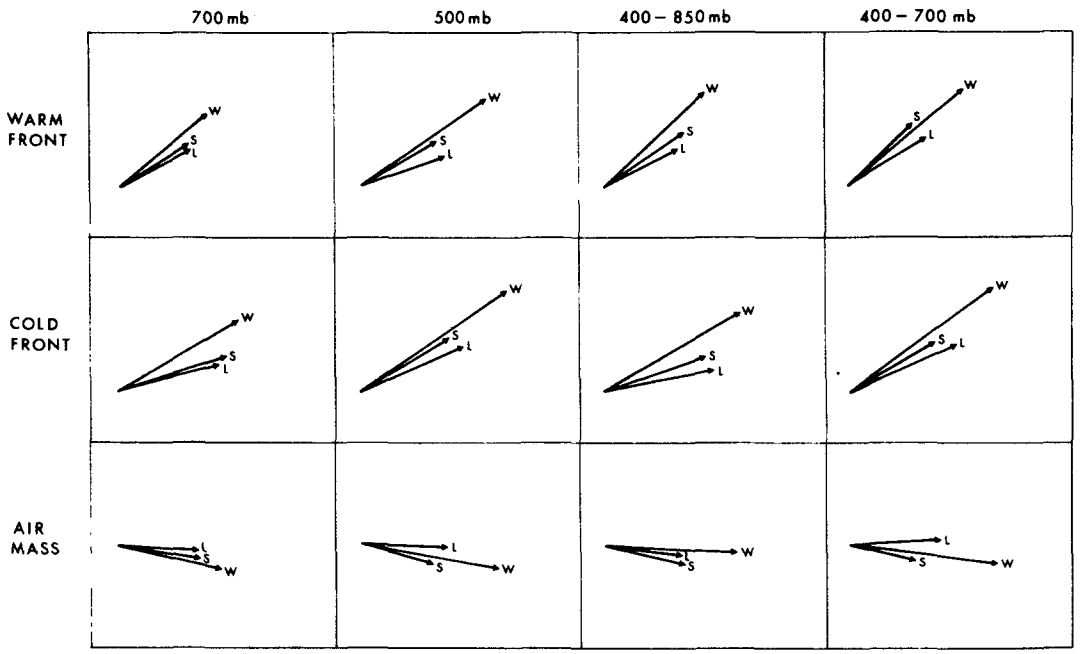

FIG. 7. Summary of echo system velocity compared with upper level wind velocity for the level categories where both direction and speed were considered (see Sections 5 and 6). All magnitudes are similarly scaled. The labels W, S and L refer to the mean wind, small echo system and large echo system velocities, respectively. North is up and east is to the right.

Even though over 200 cases were analyzed, many properties of the echo systems exhibited such a large range of values that subdivision within the echo types for comparison precluded the possibility of establishing significant differences. This was most evident when seasonal and diurnal variations correlations were attempted. Increasing the number of echo system case histories would have allowed more meaningful statistical conclusions to be reached.

Echo system movement correlation with upper level winds may be improved if the quantity of rawinsonde observations were increased. This would involve the taking of special observations within the established network and at more frequent time intervals. This, of course, is most difficult to arrange; however, an improvement in the correlation of echo system speed with upper level wind speed would be expected.

Acknowledgments. Thanks are extended to Dr. Lyle H. Horn for his constructive criticism during the conduct of this study. The authors appreciated the comments of reviewers which helped improve the paper.

Financial support for this research was provided by the National Science Foundation under Grant ATM75-03617.

REFERENCES

Austin, P. M., and R. A. Houze, Jr., 1972: Analysis of the structure of precipitation patterns in New England. *J. Appl. Meteor.*, **11**, 926–935.

Barclay, A. B., and E. Wilke, 1970: Severe thunderstorm radar echo motion and related weather events hazardous to aviation operations. NSSL Tech. Memo. No. 46, 63 pp.

Betts, A. K., and M. A. Stevens, 1974: Rainfall and radar echo statistics—Venezuelan International Meteorological and Hydrological Experiment. 1972. Res. Rep., Atmos. Sci. Dept., Colorado State University, Fort Collins, 151 pp

Cruz, L. A., 1973: Venezuelan rainstorms as seen by radar. *J. Appl. Meteor.*, **12**, 119–126.

Newton, C. W., and J. C. Fankhauser, 1964: On the movements of convective storms, with emphasis on size discrimination in relation to water-budget requirements. *J. Appl. Meteor.*, **3**, 651–668.

Wilson, J. W., 1966: Movement and predictability of radar echoes. NSSL Tech. Memo. No. 28, 30 pp.